eLIFE
elifesciences.org

# Figures and figure supplements

Munc18-1 is a dynamically regulated PKC target during short-term enhancement of transmitter release

**Özgür Genç, et al.**

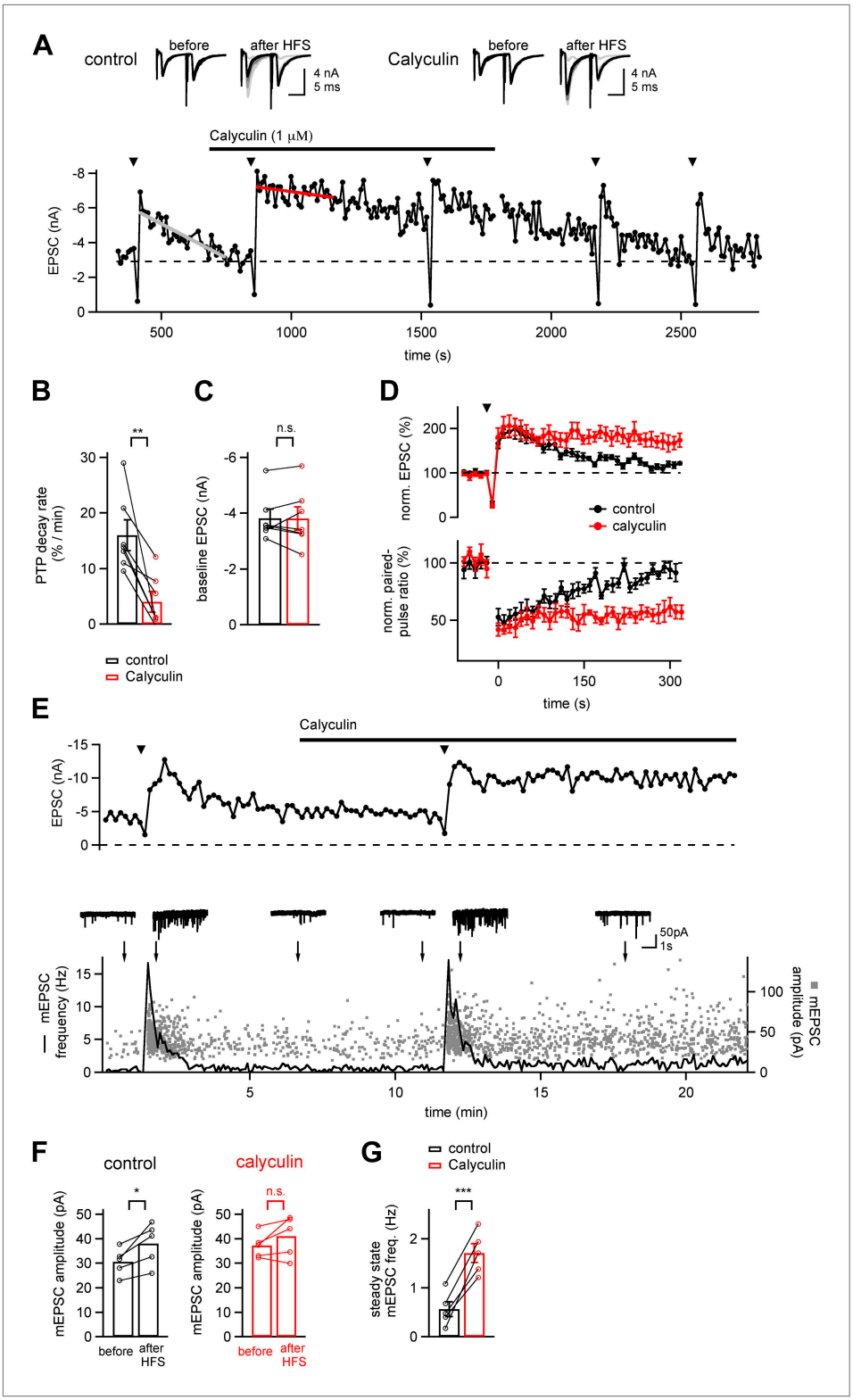


**Figure 1**. A phosphatase terminates the increased transmitter release which underlies PTP. (**A**) Time course of EPSC amplitude during the repetitive inductions of PTP (arrowheads, HFS at 100 Hz for 4 s), demonstrating the slowing of PTP decay upon acute application of phosphatase inhibitor Calyculin A. Line fits (grey and red lines) were used to estimate the decay rates of PTP. Upper inset shows example EPSCs induced by double stimuli (interval, 10 ms) before and after HFS, both for control condition (*left*) and following calyculin application (*right*).

*Figure 1. Continued on next page*

*Figure 1. Continued*

(**B** and **C**) Quantifications of PTP decay rates for control and calyculin (**B** and ***Figure 1—source data 1A***) and basal EPSC amplitudes for the two conditions (**C** and ***Figure 1—source data 1B***). (**D**) Average time courses of normalized EPSC amplitudes (*top*, PTP) and normalized paired-pulse ratio ($EPSC_2/EPSC_1$, *bottom*) in control conditions (black symbols) and in the presence of Calyculin A (red symbols), obtained in the same recordings (n = 7 cells). (**E**) Time course of evoked EPSCs (*top*) and mEPSC frequency (*bottom*, line trace) and scatter plot of individual mEPSC amplitudes (*bottom*, gray data points) as a function of experiment time, from a different example recording as the one shown in (**A**). Example mEPSC traces are shown for the time points indicated by arrows. (**F**) Quantification of average mEPSC amplitudes before PTP induction stimuli (sampled from at least five 10 s long mEPSC traces, left bars), and during a single 10 s interval immediately following PTP induction (right bars). Data for both control conditions (left) and in the presence of calyculin (right) are shown (see ***Figure 1—source data 1C***). (**G**) Quantification of the mEPSC frequency late after induction of PTP, both under control conditions, and in the subsequent presence of calyculin (1 μM) in the same cell. Note that in the presence of calyculin, the steady state mEPSC frequency was persistently increased (see ***Figure1—source data 1D***).

DOI: 10.7554/eLife.01715.003

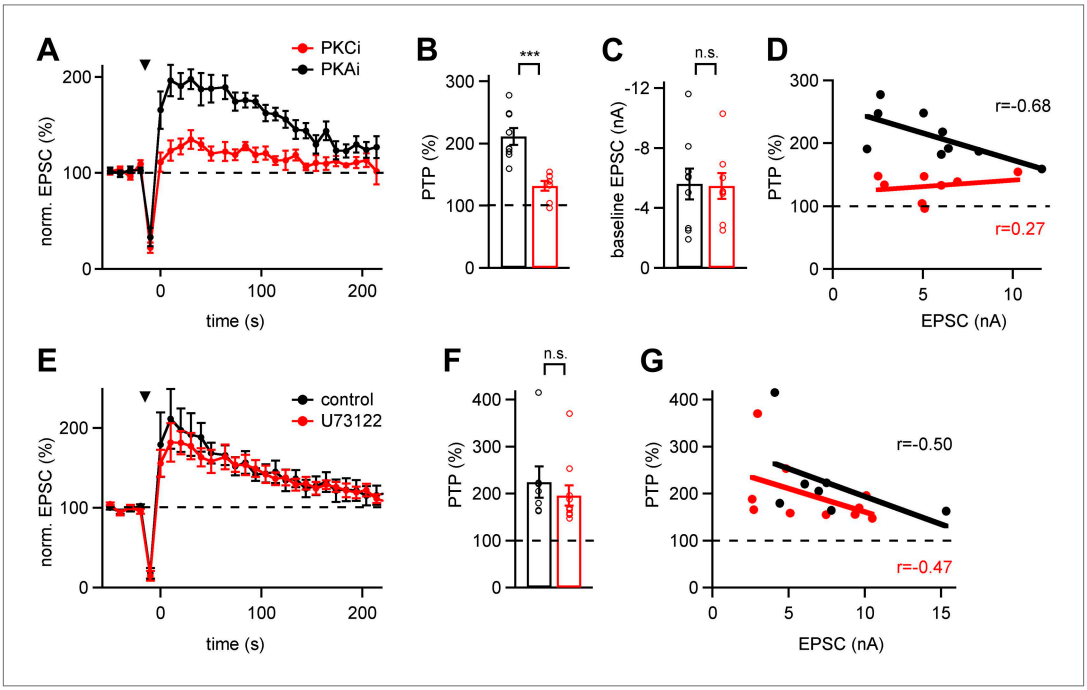


**Figure 2**. Conventional PKCs but not phospholipase-C initiate PTP. (**A**) Average time courses of normalized EPSC amplitude (PTP plots) in the presence of PKC inhibitory peptide (PKCi; red symbols, n = 8 cells) or PKA inhibitory peptide (PKAi; black symbols, n = 9 cells). Note the significant suppression of PTP by PKCi. (**B** and **C**) Quantifications of peak PTP (**B** and ***Figure 2—source data 1A***) and of baseline EPSC amplitude (**C** and ***Figure 2—source data 1B***) in the presence of PKCi (*red* symbols) and PKAi (*black*). (**D**) Plot of peak PTP amplitudes vs the basal EPSC amplitudes. Note that PTP was strongly reduced also when baseline EPSC amplitude was small. The correlation coefficients (r) are indicated. (**E**) Average PTP plots in neurons recorded after pre-incubation with the PLC blocker U73122 (red symbols; n = 10 cells), and under control conditions with 0.1% DMSO (black symbols; n = 7 cells). (**F** and **G**) Quantification of average peak PTP under control conditions and in the presence of U73122 (**F**, and ***Figure 2—source data 1C***), and plot of peak PTP amplitude vs baseline EPSC amplitude (**G**, black and red symbols, respectively). Note the absence of an effect of phospholipase-C inhibition on PTP.

DOI: 10.7554/eLife.01715.005

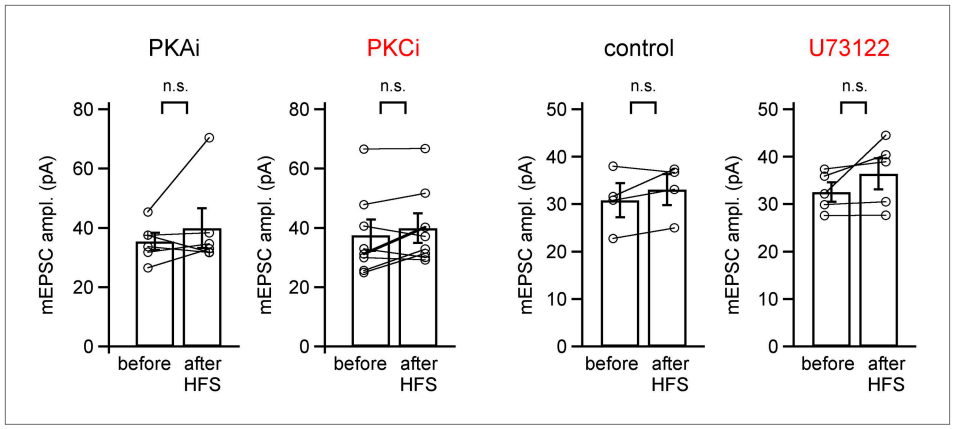


**Figure 2—figure supplement 1**. mEPSC amplitude before and after PTP induction protocols is unchanged for the PTP data sets in ***Figure 2***.

DOI: 10.7554/eLife.01715.007

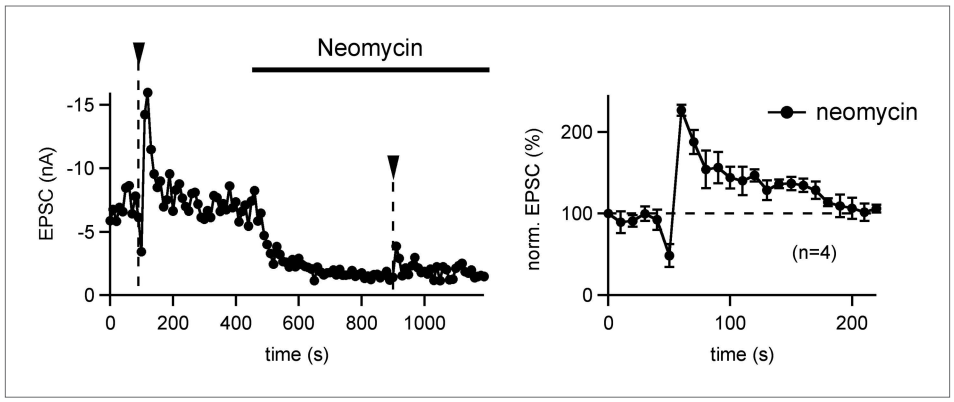


**Figure 2—figure supplement 2**. PTP is insensitive to the PLC inhibitor Neomycin.

DOI: 10.7554/eLife.01715.008

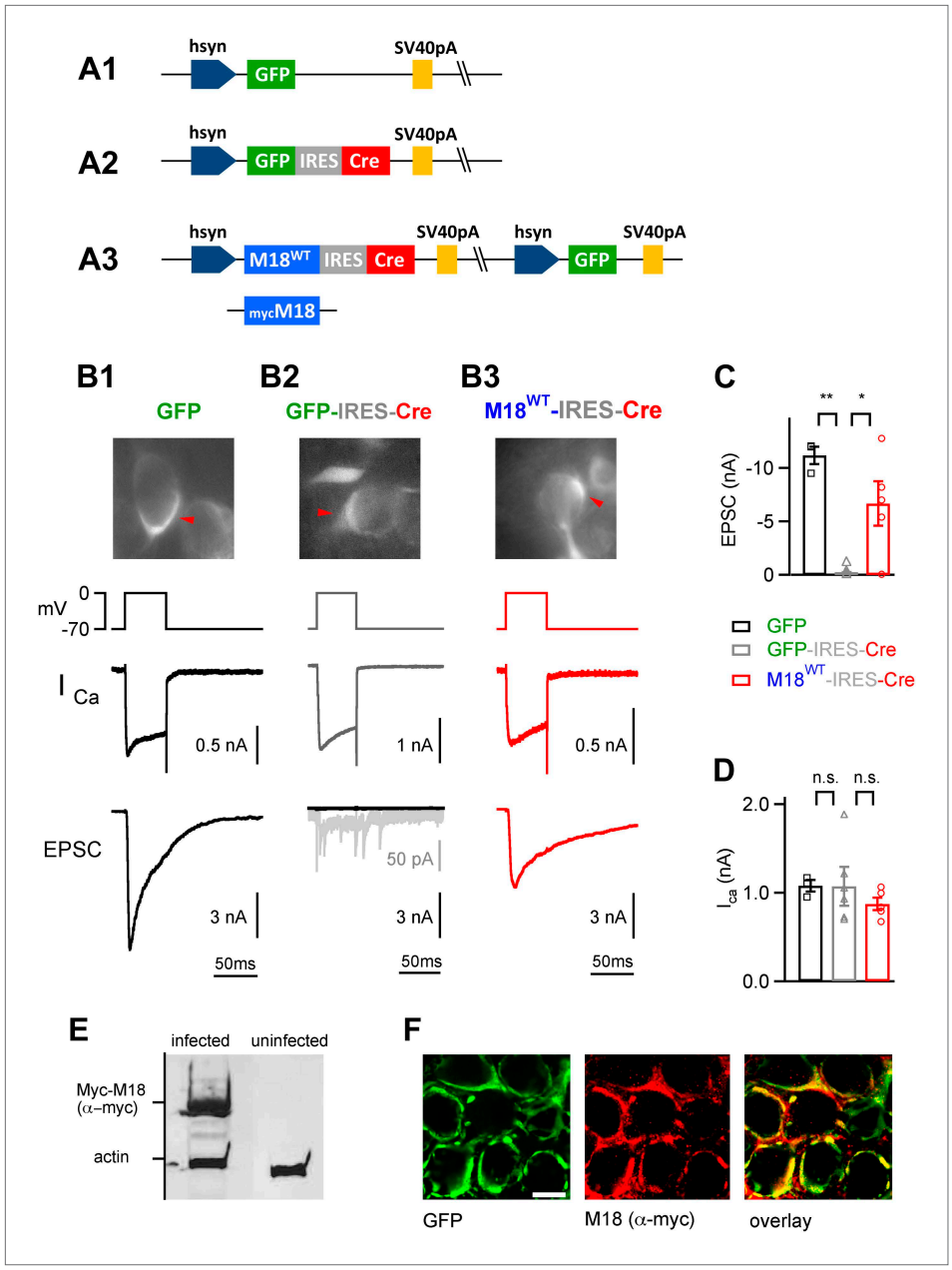


**Figure 3**. Endogenous floxed Munc18-1 can be removed and replaced by recombinant protein in vivo at the calyx of Held. (**A**) Scheme of the adenoviral DNA constructs. **A1**: control vector driving the expression of GFP alone; **A2**: control vector driving the expression of GFP-IRES-Cre; **A3**: three-protein expression vector, which drives the expression of Munc18-1 (either wild-type or myc-tagged), Cre-recombinase, and GFP from an additional cassette in the viral genomic backbone (see 'Materials and methods'). (**B**) Results from paired recordings from calyx synapses in *Munc18-1*$^{lox/lox}$ mice expressing either GFP alone (**B1**), GFP-IRES-Cre (**B2**), or M18$^{WT}$-IRES-Cre and GFP (**B3**). Shown are the corresponding GFP-positive calyces (*top*), the presynaptic voltage-clamp protocols and presynaptic $Ca^{2+}$ currents (*middle*), and the resulting postsynaptic EPSCs (*bottom*). Note the abolishment of release when Cre recombinase is expressed alone (**B2** – note remaining quantal release in grey trace with enhanced scale), and the rescue of release when Cre-recombinase is expressed together with M18$^{WT}$ protein (**B3**). These measurements were done following virus injection at P1, which we found necessary for efficient elimination of endogenous Munc18-1 protein in Cre expressing calyces. (**C** and **D**) Summary of EPSC amplitudes recorded in response to 50 ms presynaptic depolarization (**C**; see **B**), for the following conditions: expression of GFP alone (*left* bar, black data points), expression of Cre-recombinase (*middle*; grey data points), and expression of Cre-recombinase together with M18$^{WT}$ (*right*; red data points and see ***Figure3—source data 1A***). The presynaptic $Ca^{2+}$ current amplitudes were unaffected by

*Figure 3. Continued on next page*

*Figure 3. Continued*

genetic removal of Munc18-1 (**D** and ***Figure3—source data 1B***). (**E**) Adenovirus-mediated expression of myc-Munc18-1 in E2T packaging cells analyzed by SDS-PAGE and western blotting shows strong expression of recombinant protein (myc-Munc18-1, 67 kDa, actin, 43 kDa). (**F**) Immunohistochemistry of calyces of Held expressing the myc-tagged M18 construct in a P11 *Munc18*$^{lox/lox}$ mouse after injection at P1. Antibodies against GFP (*left*, green channel) and c-myc (*middle*, red channel) were used; the overlay image is shown on the right. Scale bar, 10 µm.

DOI: 10.7554/eLife.01715.009

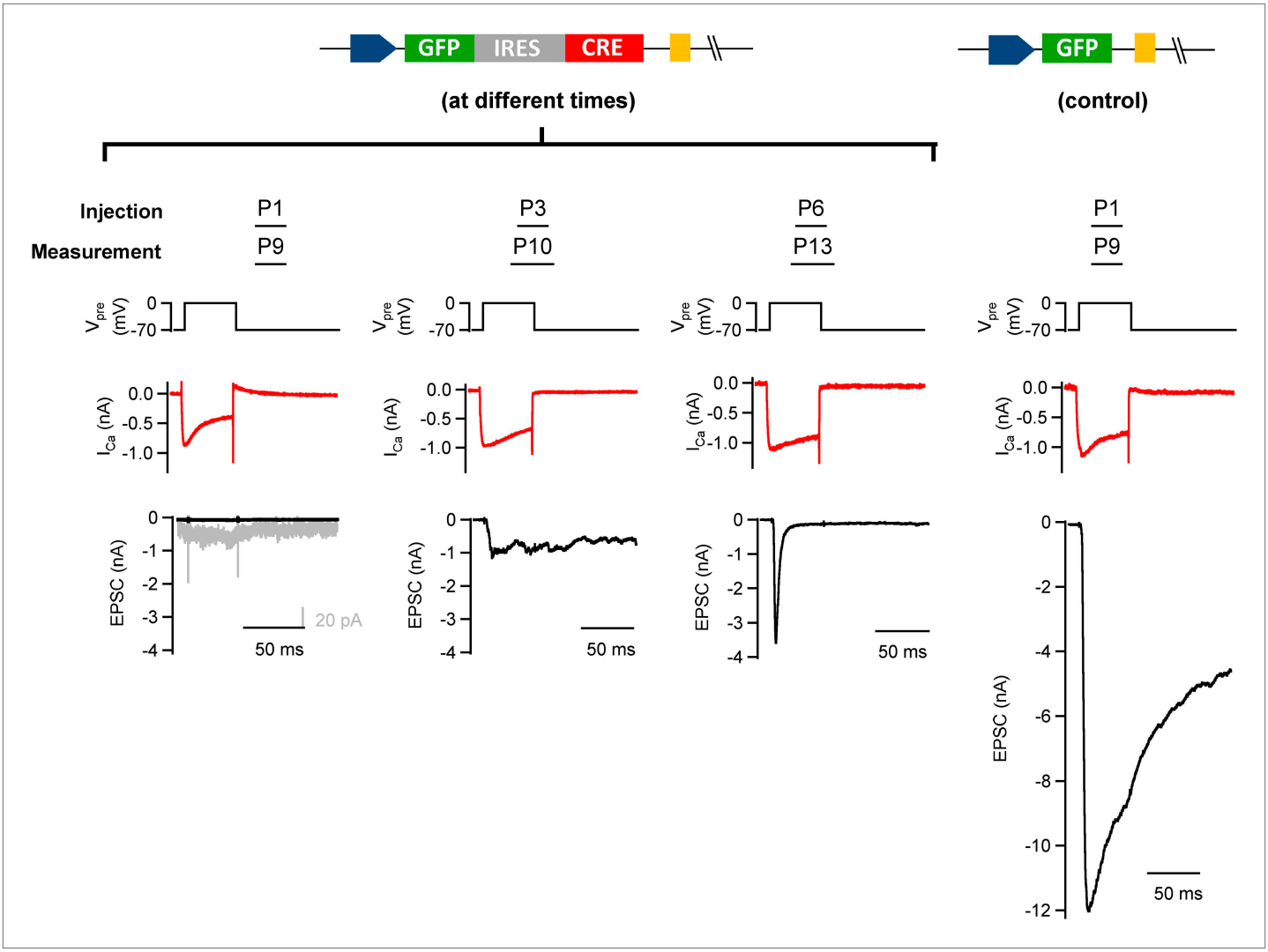


**Figure 3—figure supplement 1**. Early postnatal Cre expression was necessary for complete removal of endogenous Munc18-1.

DOI: 10.7554/eLife.01715.011

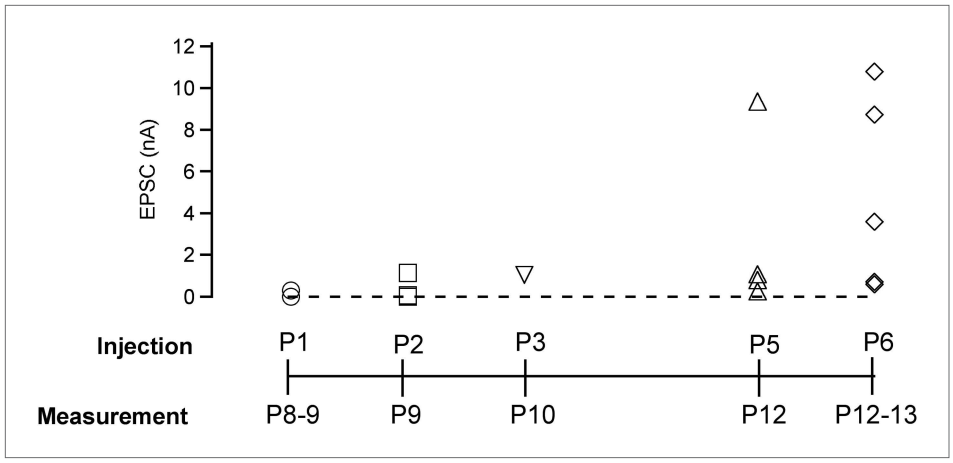


**Figure 3—figure supplement 2**. Early postnatal Cre expression was necessary for complete removal of endogenous Munc18-1: summary.
DOI: 10.7554/eLife.01715.012

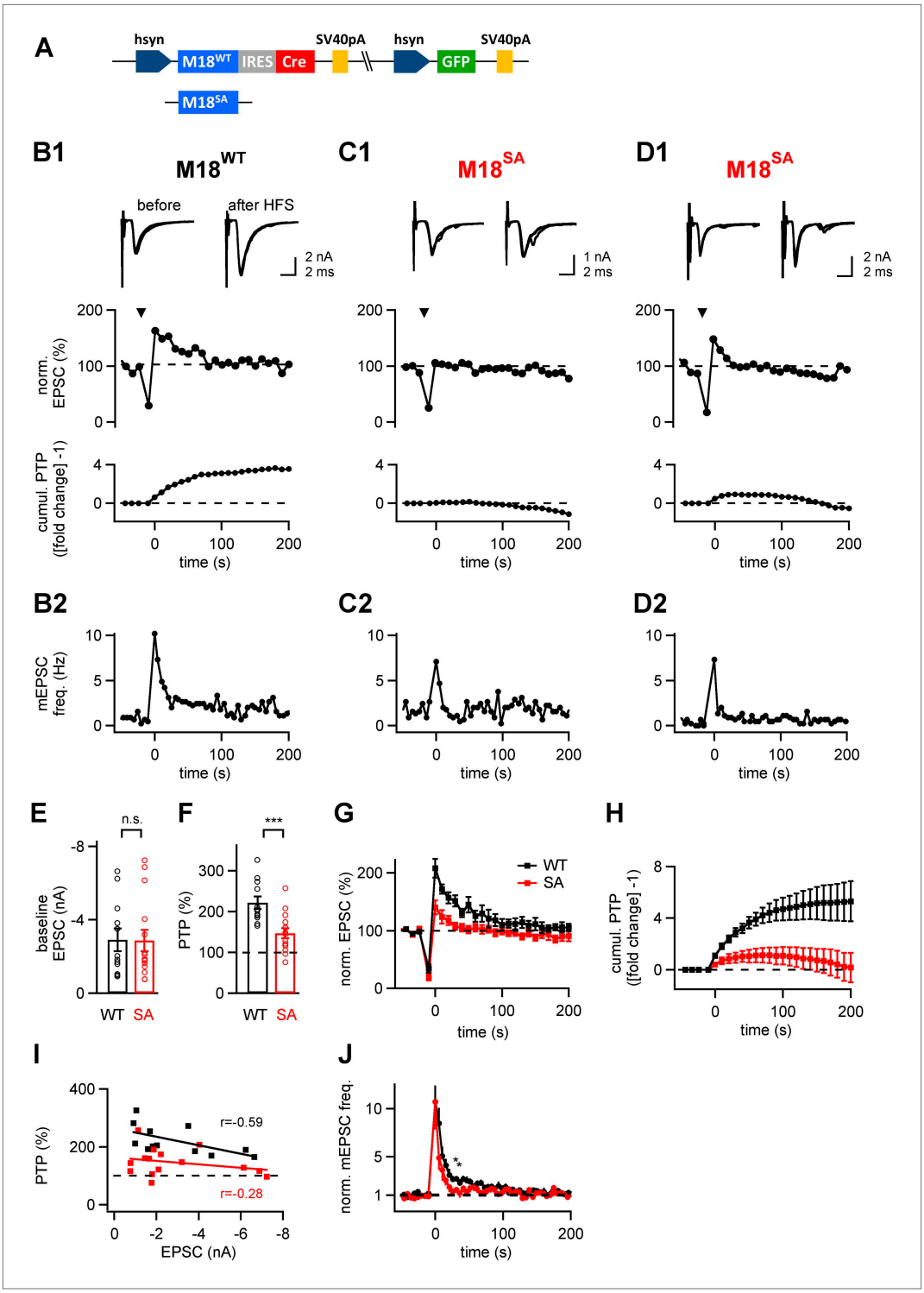


**Figure 4**. The PKC phosphorylation sites of Munc18-1 are necessary for the expression of post-tetanic potentiation, PTP. (**A**) Scheme of the three-protein expression constructs used for the experiments shown in this figure. Either wild-type Munc18-1 ($M18^{WT}$) or the PKC-phosphorylation site triple mutation (S306A, S312A, S313A; $M18^{SA}$) were expressed together with Cre-recombinase and GFP. (**B-D**) PTP from three example cells, one rescued with wild-type Munc18-1 ($M18^{WT}$, **B1**, **B2**), the other two rescued with the PKC-phosphorylation site deficient mutant ($M18^{SA}$; **C1**, **C2** and **D1**, **D2**). From *top* to *bottom*, individual EPSC traces before (*left*) and after (*right*) PTP; plots of relative EPSC amplitudes vs time (PTP plot), and plots of cumulative PTP vs time.

*Figure 4. Continued on next page*

*Figure 4. Continued*

Note that PTP was absent (**C1**) or smaller in synapses rescued with $M18^{SA}$; when substantial PTP remained, it decayed more rapidly (**D1**, *middle*). The panels in (**B2**–**D2**) plot the mEPSC frequency for the corresponding cells on the same time scale. (**E** and **F**) Summary plots of baseline EPSC amplitudes (**E** and ***Figure 4—source data 1A***) and of peak PTP (**F** and ***Figure 4—source data 1B***) for synapses rescued with wild-type Munc18-1 ($M18^{WT}$; *black* symbols) and with the mutant form ($M18^{SA}$; *red* symbols). (**G**) Average PTP plots for synapses rescued with $M18^{WT}$ (*black* symbols) and $M18^{SA}$ mutant (*red*; n = 12 and n = 15 cells, respectively). (**H**) Average cumulative PTP for synapses rescued with $M18^{WT}$ (*black* symbols) and $M18^{SA}$ mutant (*red*; n = 12 and n = 13 cells, respectively). (**I**) Plot of peak PTP amplitudes vs the basal EPSC amplitudes shows that PTP was reduced over the entire range of basal EPSC amplitudes. The correlation coefficients (r) are indicated. (**J**) Normalized average mEPSC frequency following PTP induction trains, recorded at synapses rescued with $M18^{WT}$ (black) and $Munc18^{SA}$ (red). In the range of 0–60 s, significance was tested by paired t-test. Two data points at around 30–40 s were found to be significantly different between the two conditions ($p<0.05$; see star symbols). Thus, Munc18-1 phosphorylation was not necessary for late release in the first 10 s interval after PTP induction, but probably supported some late enhanced mEPSC frequency, in agreement with the calyculin data in ***Figure 1E***.

DOI: 10.7554/eLife.01715.013

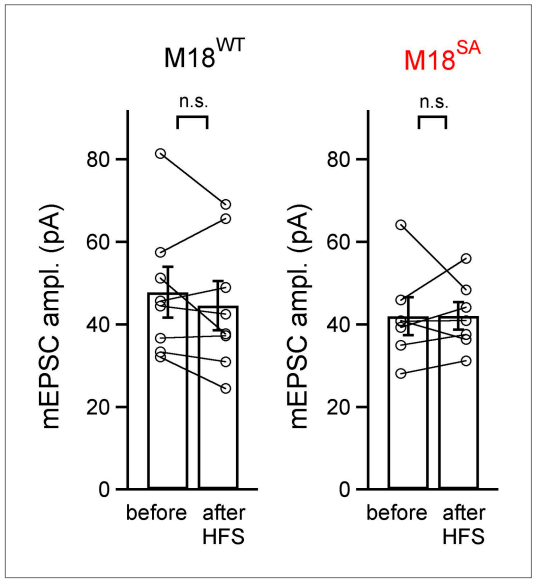


**Figure 4—figure supplement 1**. mEPSC amplitude before and after PTP induction is unchanged in rescue experiments with wild-type or PKC-insensitive Munc18-1 mutant.

DOI: 10.7554/eLife.01715.015

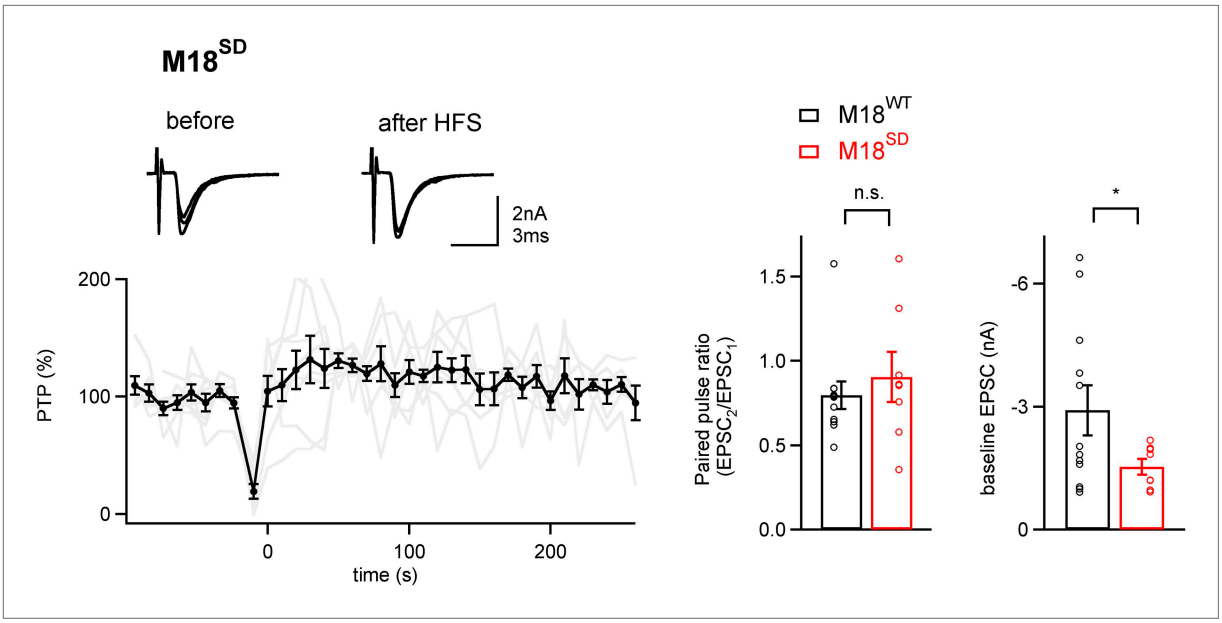


**Figure 4—figure supplement 2**. PTP is blocked in synapses rescued by a phosphomimetic Munc18-1 mutant.
DOI: 10.7554/eLife.01715.016

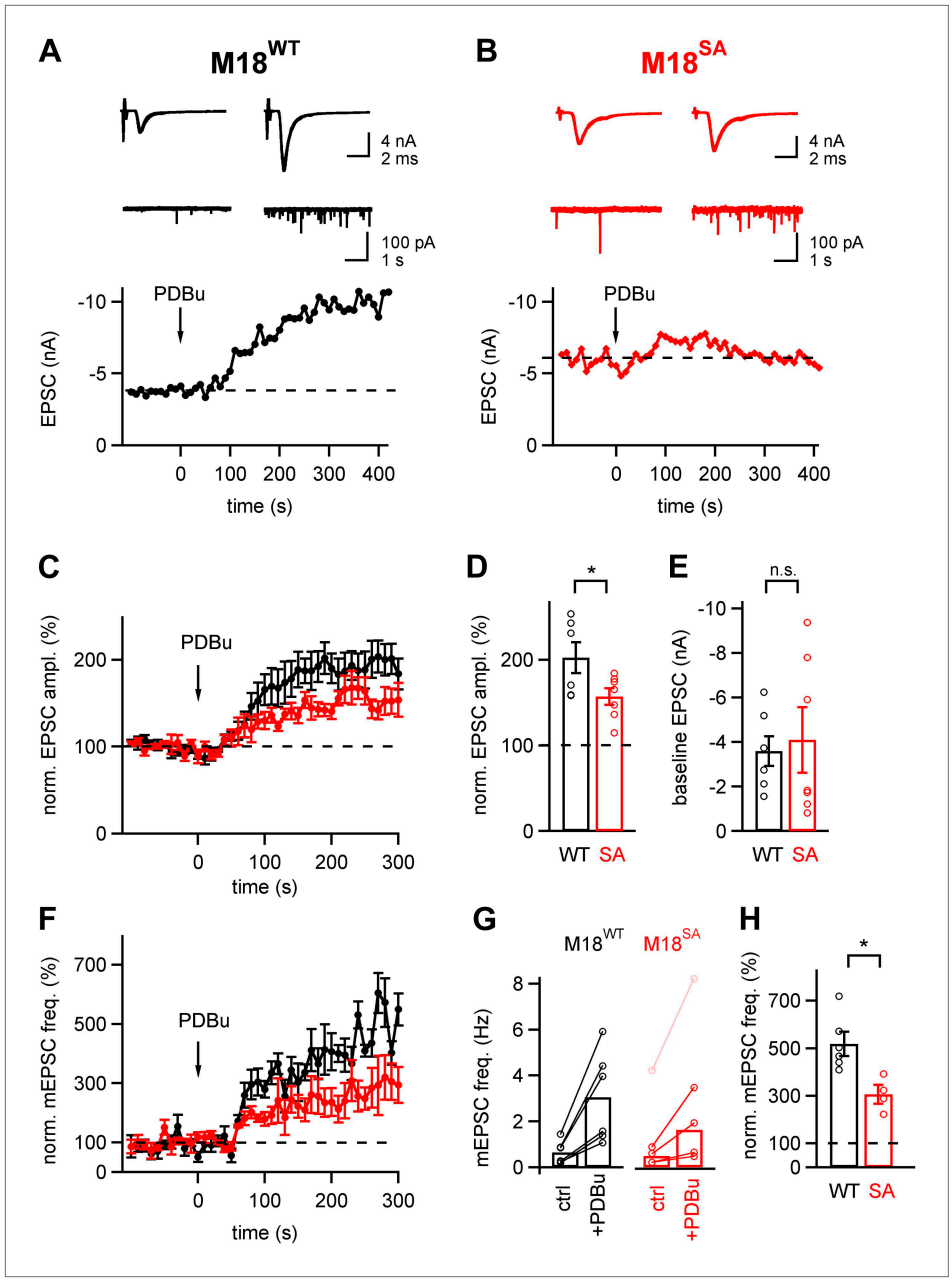


**Figure 5**. About half of the phorbol ester potentiation of evoked and spontaneous EPSC depends on PKC phosphorylation of Munc18-1. (**A** and **B**) Evoked EPSC traces (*top*) and spontaneous EPSCs (*middle*) are shown both before (*left*) and after (*right*) application of 1 μM PDBu to the slice. The *bottom* panels show time plots of evoked EPSC amplitudes and their potentiation by PDBu. Data for a $M18^{WT}$ rescued synapse (**A**) and for a $M18^{SA}$ rescued synapse (**B**) are shown. (**C**) Average time courses of normalized EPSC amplitudes during PDBu potentiation for synapses rescued with $M18^{SA}$ (*red* symbols) and $M18^{WT}$ (black, n = 7 and n = 6 cells, respectively). (**D** and **E**) Quantifications of the average and individual values for EPSC potentiation (**D**, ***Figure 5—source data 1A***) and for the baseline EPSC amplitudes (**E**, ***Figure 5—source data 1B***) in synapses rescued with $M18^{SA}$ (*red*) and with $M18^{WT}$ (*black*). Note that ~half of the potentiation of evoked EPSC amplitudes depended on an intact Munc18-1 phosphorylation site. (**F**) Average time courses of normalized spontaneous EPSC frequency before and after PDBu application, both for synapses rescued with $Munc18^{SA}$ (*red* symbols) and with $M18^{WT}$ (*black*; n = 4 and 6, respectively). (**G**) Quantification of absolute mEPSC frequencies before and after PDBu application, for synapses rescued with $M18^{WT}$ and $M18^{SA}$. For the $M18^{SA}$ data, an outlier data point with an unusually high baseline frequency (4 Hz; pink symbols) was removed when calculating the average absolute mEPSC frequencies (see ***Figure5—source data 1C***). (**H**) Average relative potentiation of mEPSC frequency under both conditions. Note that about half of the potentiation of spontaneous release depends on the PKC phosphorylation of Munc18-1 (see ***Figure5—source data 1D***).

DOI: 10.7554/eLife.01715.017

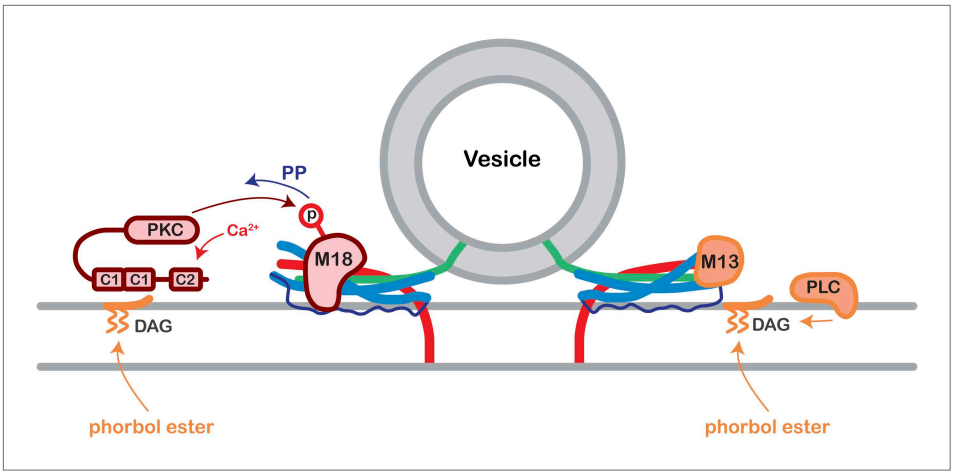


**Figure 5—figure supplement 1**. Model of Munc18-1 PKC phosphorylation and de-phosphorylation and its effect on presynaptic plasticity.
DOI: 10.7554/eLife.01715.019